**ICE-PENETRATING IMPACTS: INSIGHTS FROM HYPERVELOCITY IMPACT EXPERIMENTS AND GALILEO IMAGE MAPPING OF EUROPA** Kate C. Scheider and Rónadh Cox, Department of Geosciences, Williams College, Williamstown MA 01267; *rcox@williams.edu*

**Introduction:** Where an ice crust overlies water, as it seems to on Europa, some impactors may breach it completely. Chaos areas may provide a record of such events. Hypervelocity impact experiments at the NASA Ames Vertical Gun Range (AVGR) reveal some of the mechanics of ice-penetrating impacts; and combined with crater-count data from high-resolution images (<50 m/pixel) surrounding the large chaos area Thera Macula, provide an initial model for the geomorphologic expression of penetrating impacts.

**Impact experiments:** We report the results of two AVGR experiments. Impact velocities were 5.5 and 5 km/sec, and the targets consisted of ice plates (70 $cm^2$, 2.3 and 1.5 cm-thick respectively) overlying 25 cm of water in a tank 81 $cm^2$ x 40 cm deep. Both shots overwhelmed the target container and therefore edge effects are a problem: the design of future experiments will be modified to address this. But the data—from 1000 frame/sec imagery of the impacts—provide useful initial information about the ejecta dynamics.

Immediately on impact, an inverted ejecta cone formed at 60° to the target surface. Simultaneously, radial and concentric fractures propagated through the ice. The base of the ejecta cone was displaced upward by growth of a cupola [1] of water and spalled ice, which thereafter dominated the event sequence. Smaller fragments at the top of the cupola traveled at 80-90° up through the ejecta cone. As the cupola expanded, bulging water pushed the ice up and outward from beneath. The breaking ice hinged along concentric fractures, creating plates of successively larger sizes as the hinging progressed outward. Radial fractures were so widely spaced at distance from the impact site that the outermost spall plates were too large to be ejected; instead, they fell back, fracturing into smaller plates on impact with the water. The sides of the cupola evolved to form an ejecta curtain with angles 60-90° before collapsing. As the cupola disintegrated, a water spout (the central peak [2]) formed, and reached ≈0.75 m height before collapsing, generating gravity waves on the water surface.

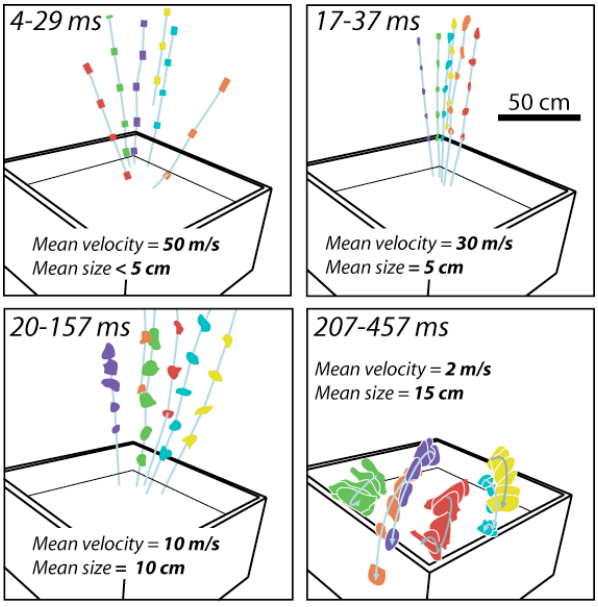


Fig. 1: Trajectories, average velocities, and average sizes for representative ejecta. Time range in each panel is in milliseconds post-impact, and the average velocity and average size (maximum dimension) for the measured population is given in each case. The ejection velocity decreased and the ejecta size increased with time. The maximum ejection velocity, in the earliest stages, was only ≈1% of the impact velocity; and the lowest ejection angles were ≈60°.

Ejecta velocities were low: the fastest moving fragments traveled at ≈50 m/sec, only 1% of the impact velocity (Fig. 1). In contrast, ejecta from hypervelocity crater-forming impacts into solid ice targets travel at 66-90% of the impact velocity [3], and those into porous ice or ice-silicate travel at 20-50% [4]. The maximum ejection angle $V_{e\ max}$ was almost 90° for the fastest-moving and smallest fragments, and even the lowest angles were close to 60° (for the late, slow-moving spall plates). Again, these contrast strongly with both solid ice ($V_{e\ max}$ 14-68° [3]) and porous ice targets ( $V_{e\ max}$ 30-50° [4]). These results are consistent with hydrocode modeling, which predicts slower-moving ejecta for ice-penetrating impacts [5]. Ejecta landed both on the exposed water surface and outside the impact zone. Fragments landing on the water were tossed by waves, reoriented, and in some cases tilted.

**Implications for planetary impacts:** If ice-penetrating impacts puncture the crust and expose an underlying ocean, then the impact site will look nothing like a crater. Rather, it may resemble a jagged-edged hole, with ejecta fragments sitting in a matrix of refrozen liquid [6, 7]. The hole will be surrounded by a secondary impact field; but because $V_e$ is so much lower than from impacts into solid ice, the secondary craters will be much smaller than those associated with non-penetrating impacts of the same energy. And because the ejection trajectories are so much steeper, (a) a large proportion of the ejecta will land within the impact site, potentially forming rafts in the exposed liquid; and (b) the radius of the secondary field will be smaller than for a comparable solid-target impact.

**Chaos areas on Europa are candidates for ice-penetrating impact sites:** Chaos areas are sites where the ice crust has been destroyed, and where liquid was exposed and mixed with pieces of the fragmented ice crust before freezing. Most chaos areas approximately equidimensional, with abrupt edges; and low-velocity impact experiments show that penetrating impacts produce morphologic outcomes with many of the features of chaos terrain [6, 7]. If chaos areas do represent impact sites, then they should have secondary crater fields associated with them.

**Resolving secondary crater fields for ice-penetrating impacts:** Although the secondary fields about large impact sites such as Pwyll and Tyre are clearly visible in the regional images of resolution 150-300 m/pixel, this is because the median crater size in these fields is of order ≈1 km [8, 9]. Reliable feature recognition drops off rapidly below 4 pixels diameter; and secondary-crater fields are not resolvable around smaller impact craters on Europa for this reason. Likewise—because of the order of magnitude difference in ejection velocity and factor of 2-3 difference in ejection angle—the much smaller secondary craters from penetrating impacts are therefore unlikely to be evident at regional imaging scales. Mapping such fields requires high-resolution images (<100 m/pixel).

**Mapping secondary craters around Thera Macula:** No large chaos areas (with the exception of Conamara Chaos, which lies within the Pwyll secondary crater field) are imaged at better than 250 m/pixel; but as luck would have it, there are three high-resolution mosaics distributed evenly around Thera Macula (Fig. 2) which—while they are not sufficiently extensive to allow us to fully map a secondary crater field—allow us to test whether small craters are distributed preferentially with respect to the chaos area [7].

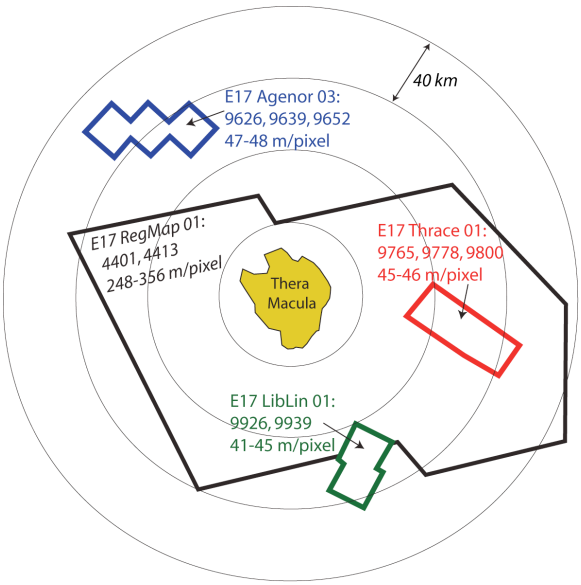


Fig. 2. Distribution of Galileo images in the Thera Macula region. Circles show distance from Thera's centre in 1-radius increments. The outlines of the regional images and of the high-resolution image mosaics are shown. The data in Fig. 3 were derived only from the three high-resolution mosaics. Colours keyed to Fig. 3.

Small-crater densities decrease exponentially as a function of distance from the centre of Thera (Fig. 3), suggesting that Thera is the source of the impactors. We do note, however, that because of the restricted high-resolution coverage, these data represent only ≈8% of the area between 3 and 7.5 Thera radii.

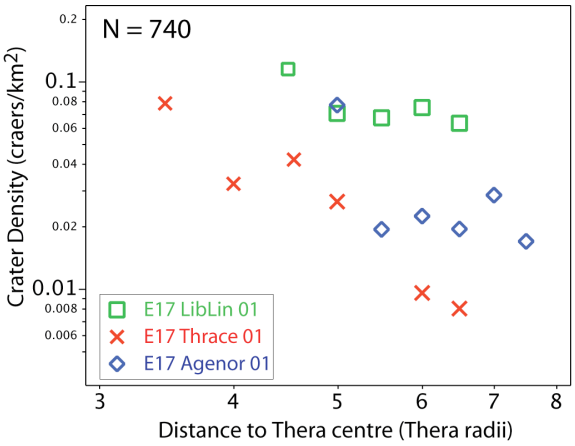


Fig.3. Crater densities mapped from high-resolution (41-48 m/pixel) image mosaics in the vicinity of Thera macula, as a function of distance from the chaos area centre. The decrease in small-crater density away from Thera's centre suggests that Thera is the source of the crater-forming debris.

If chaos areas do represent impact sites, their secondary crater fields will not be mappable on the current image database. Thera, at ≈80 km equivalent circle diameter, is more one of the largest chaos areas on Europa, more than 3 times larger than Pwyll and twice the size of Tyre. But the median size of small craters on the high-resolution images is only 400 m: less than half the size of the Pwyll and Tyre secondary craters. Impact experiments will continue to expand our understanding of impacts into layered ice-water systems, but resolving these features on Europa needs better image coverage than we presently have.

**References:** [1] Ormo J. et al. (2006) *Meteoritics and Planet. Sci. 41*, 1605-1612. [2] Gault D. E. and Sonett C. P. (1982) *Geol. Soc. Amer. Spec. Pap. 190*, 69-92. [3] Arakawa M. (1999) *Icarus 142*, 34-45. [4] Arakawa M. et al. (2002) *Icarus 158*, 516-531. [5] Moore J. M. et al. (1998) *Icarus 135*, 127-145 [6] Cox R. et al. 2005 *LPS XXXVI, Abstr. # 2101*. [7] Cox R. et al. (in press) *Icarus*. [8] Bierhaus B. 2006 *Workshop on Surface Ages and Histories: Abstr. #. 6028*. [9] Bierhaus B. et al. 2005 *LPS XXXVI, Abstr. #. 2386*.